ARE REGISTRATION ERRORS ALWAYS BAD FOR SUPER-RESOLUTION?

Guilherme H. Costa and José C. M. Bermudez

Department of Electrical Engineering
Federal University of Santa Catarina
Florianópolis, SC - Brazil

ABSTRACT

The super-resolution reconstruction (SRR) of images is an ill posed problem. Traditionally it is treated as a regularized minimization problem. Moreover, one of the major problems concerning SRR is its dependence on an accurate registration. In this work we show that a certain amount of registration error may, in fact, be beneficial for the performance of the Least Mean Square SRR (LMS-SRR) adaptive algorithm. In these cases, the regularization term can be avoided and computational cost is reduced, an important advantage in real-time SRR applications.

Index Terms— Image reconstruction, image registration, LMS, adaptive estimation

1. INTRODUCTION

An approach to improve digital image quality which has attracted large interest in the last decade uses super-resolution reconstruction (SRR). SRR consists basically of combining multiple low-resolution (LR) images of the same scene or object to form a higher resolution image. This problem is traditionally formulated as a minimization problem. However, SRR frequently leads to ill-posed inverse problems because of ill-conditioned blur operators or insufficient number of LR images. For this reason, a regularization term is usually considered in the minimization problem [1, 2, 3].

The Least Mean Square (LMS-SRR) algorithm proposed in [3] to solve the SRR problem is an interesting solution for real-time applications, such as SRR of video sequences, due to the simplicity of the stochastic gradient approximation. The results in [3] show a performance improvement when LMS is regularized (leading to the R-LMS algorithm).

One of the major issues regarding SRR algorithms is their dependence on an accurate registration. Registration errors have always been regarded as detrimental to the SRR performance, and several works have proposed algorithms that are robust to the effects of such errors [2, 4, 5]. This robustness usually comes at the cost of an increase in computational complexity. More recently, a new algorithm has been proposed which is robust to registration and admits a fast implementation for global translational image motions [6]. However, even under these conditions its computational cost and memory requirements are not competitive with [3]. Finally, we have verified in our experiments that moderate levels of registration error in the LMS-SRR may improve the algorithm's performance and render regularization unnecessary.

In this work we present a study of the equivalence between the effects of registration errors and regularization in the performance of the LMS-SRR algorithm. We show that when only one iteration of the LMS-SRR is performed by time sample, moderate levels of registration errors may improve the algorithm performance. In this case, the registration error acts like a regularization, and thus the regularization term can be avoided, saving computational resources. More information on the design of the LMS-SRR using different number of iterations by time sample can be found in [7]. Our analysis considers the occurrence of whole-image translational movement only. This is the simplest case to handle and is representative of several practical applications [6, 8].

In Section 2, we briefly review the LMS-SRR algorithm and its regularized version [3]. In Section 3, we present the algorithm analysis and study the influence of both the registration errors and the regularization term on the image estimation error. In Section 4 we present simulation results which corroborate the conclusions reached in Section 3. Finally, in Section 5 we conclude this work.

e-mail:holsbach@eel.ufsc.br; j.bermudez@ieee.org. This work has been supported in part by CNPq under grants 141456/2003-5 and 308095/2003-0.

2. THE LMS-SRR ALGORITHM

Hereafter, bold lowercase letters denote column vectors and bold uppercase letters denote matrices. The variable t is integer and indexes discrete-time samples of images and operators. We refer to the observed (low-resolution) images as LR images, and to both the original (desired) and the reconstructed high-resolution images as HR images.

2.1. The signal models

Given the $N \times N$ matrix representation of an LR (observed) digital image $\mathbf{Y}(t)$ and an $M \times M$ ($M > N$) matrix representation of the original HR digital image $\mathbf{X}(t)$, the acquisition process can be modelled as [1]

$$\mathbf{y}(t) = \mathbf{D}(t)\mathbf{x}(t) + \mathbf{e}(t)\,, \tag{1}$$

where vectors $\mathbf{y}(t)$ ($N^2 \times 1$) and $\mathbf{x}(t)$ ($M^2 \times 1$) are the lexicographic representations of the degraded and original images, respectively, at the discrete time instant t. The $N^2 \times M^2$ matrix $\mathbf{D}(t)$ models the degradation due to sub-sampling and blurring, and is assumed known. The $N^2 \times 1$ vector $\mathbf{e}(t)$ models the observation (electronic) noise, which is assumed stationary in space and time, statistically independent of $\mathbf{y}(t)$ and $\mathbf{x}(t)$, white, Gaussian, with zero mean and with space autocorrelation matrix $\mathbf{R_e} = \mathrm{E}\{\mathbf{e}(t)\mathbf{e}^{\mathrm{T}}(t)\} = \sigma_e^2\mathbf{I}$. σ_e^2 is assumed to be determined from camera tests [9].

The dynamics of the input signal is modelled by

$$\mathbf{x}(t) = \mathbf{G}(t)\mathbf{x}(t-1) + \mathbf{s}(t)\,, \tag{2}$$

where $\mathbf{G}(t)$ is the warp matrix that describes the relative displacement from $\mathbf{x}(t-1)$ to $\mathbf{x}(t)$. Vector $\mathbf{s}(t)$ models the innovations in $\mathbf{x}(t)$, and thus includes the contributions of outliers to the reconstructed image.

2.2. The LMS-SRR Adaptive Algorithm

The LMS-SRR algorithm attempts to minimize the mean-square error (MSE) $\mathrm{E}\{\|\boldsymbol{\epsilon}(t)\|^2\}$ [3], where $\boldsymbol{\epsilon}(t) = \mathbf{y}(t) - \mathbf{D}(t)\hat{\mathbf{x}}(t)$, $\hat{\mathbf{x}}(t)$ is the estimate of $\mathbf{x}(t)$ and $\mathrm{E}\{\cdot\}$ denotes statistical expectation. The cost function is defined as $\mathbf{J}_{\mathrm{MS}}(t) = \mathrm{E}\{\|\boldsymbol{\epsilon}(t)\|^2 \,|\, \hat{\mathbf{x}}(t)\}$. The steepest descent update of $\hat{\mathbf{x}}(t)$ is in the negative direction of the gradient

$$\nabla \mathbf{J}_{\mathrm{MS}}(t) = \frac{\partial \mathbf{J}_{\mathrm{MS}}(t)}{\partial \hat{\mathbf{x}}(t)} = -2\mathbf{D}^{\mathrm{T}}(t)\{\mathrm{E}[\mathbf{y}(t)] - \mathbf{D}(t)\hat{\mathbf{x}}(t)\} \tag{3}$$

and thus $\hat{\mathbf{x}}_{k+1}(t) = \hat{\mathbf{x}}_k(t) - (\mu/2)\nabla \mathbf{J}_{\mathrm{MS}}(t)$. Notice that the performance surface $\mathbf{J}_{\mathrm{MS}}(t)$ is defined for a specific time instant t.

The LMS-SRR algorithm is the stochastic version of the steepest descent algorithm. Using the instantaneous estimate of (3) yields

$$\hat{\mathbf{x}}_{k+1}(t) = \hat{\mathbf{x}}_k(t) + \mu \mathbf{D}^{\mathrm{T}}(t)[\mathbf{y}(t) - \mathbf{D}(t)\hat{\mathbf{x}}_k(t)]\,, \tag{4}$$

which is the LMS-SRR update equation for a fixed t and $k = 1, \ldots, K$. The time update of (4) is based on the signal dynamics (2), and performed by $\hat{\mathbf{x}}_0(t+1) = \mathbf{G}(t+1)\hat{\mathbf{x}}_K(t)$. Using the latter expression in (4), solving for a time recursion in $\hat{\mathbf{x}}_K(t)$, and dropping the subscript K for simplicity, we have the LMS-SRR recursion [8]

$$\hat{\mathbf{x}}(t) = \mathbf{A}^K(t)\mathbf{G}(t)\hat{\mathbf{x}}(t-1) + \mu \sum_{n=0}^{K-1} \mathbf{A}^n(t)\mathbf{D}^{\mathrm{T}}(t)\mathbf{y}(t)\,, \tag{5}$$

where $\mathbf{A}(t) = [\mathbf{I} - \mu \mathbf{D}^{\mathrm{T}}(t)\mathbf{D}(t)]$.

2.3. The LMS-SRR algorithm considering registration errors

Registration errors can be modelled by a change in $\mathbf{G}(t)$ as [2]

$$\hat{\mathbf{G}}(t) = \mathbf{G}(t) + \boldsymbol{\Delta}\mathbf{G}(t)\,, \tag{6}$$

where $\hat{\mathbf{G}}(t)$ is the estimated warp matrix, and $\boldsymbol{\Delta}\mathbf{G}(t)$ is the registration error matrix. Thus, considering estimation errors, the LMS-SSR algorithm becomes

$$\hat{\mathbf{x}}(t) = \mathbf{A}^K(t)\hat{\mathbf{G}}(t)\hat{\mathbf{x}}(t-1) + \mu \sum_{n=0}^{K-1} \mathbf{A}^n(t)\mathbf{D}^{\mathrm{T}}(t)\mathbf{y}(t)\,. \tag{7}$$

2.4. The regularized LMS-SRR algorithm

The regularized LMS-SRR (R-LMS-SRR) algorithm is proposed in [3] and can be derived from the cost function

$$\mathbf{J}_{\mathrm{MS_R}}(t) = \mathrm{E}\{\|\boldsymbol{\epsilon}_r(t)\|^2 \,|\, \hat{\mathbf{x}}(t)\}\,, \tag{8}$$

where

$$\boldsymbol{\epsilon}_r(t) = \|\mathbf{y} - \mathbf{D}(t)\hat{\mathbf{x}}(t)\|^2 + \lambda\|\mathbf{S}\hat{\mathbf{x}}(t)\|^2\,, \tag{9}$$

and $\mathbf{S}$ is a high-pass filter.

Following the same steps as in Section 2.2 we obtain the R-LMS-SRR recursion, which for $\boldsymbol{\Delta}\mathbf{G}(t) = \mathbf{0}$ is given by

$$\begin{aligned}\hat{\mathbf{x}}(t) &= [\mathbf{A}(t) + \lambda \mathbf{S}^{\mathrm{T}}\mathbf{S}]^K \mathbf{G}(t)\hat{\mathbf{x}}(t-1) \\ &\quad + \mu \sum_{n=0}^{K-1} [\mathbf{A}(t) + \lambda \mathbf{S}^{\mathrm{T}}\mathbf{S}]^n \mathbf{D}^{\mathrm{T}}(t)\mathbf{y}(t)\,. \end{aligned} \tag{10}$$

3. THE ANALYSIS

In this section we present a study comparing the LMS-SRR algorithm with registrations errors with the R-LMS-SRR without registration errors ($\boldsymbol{\Delta}\mathbf{G}(t) = \mathbf{0}$). The study is based on the second order moment of the HR image estimation error $\mathbf{v}(t) = \hat{\mathbf{x}}(t) - \mathbf{x}(t)$.

An analytical model for the stochastic behavior of the LMS-SRR with registration errors has been presented in [8, 10]. This model includes a recursion for the second order moment of the estimation error $\mathbf{v}(t)$. Considering $K = 1$ in (7), the recursion is given by

$$\begin{aligned}\mathbf{K}_{\mathrm{LMS}}(t) &= \mathbf{A}(t)\mathbf{G}(t)\mathbf{K}_{\mathrm{LMS}}(t-1)\mathbf{G}^{\mathrm{T}}(t)\mathbf{A}(t) \\ &\quad + \mathbf{A}(t)\mathbf{G}(t)\,\mathrm{E}[\mathbf{v}(t-1)\hat{\mathbf{x}}^{\mathrm{T}}(t-1)]\,\mathrm{E}[\boldsymbol{\Delta}\mathbf{G}^{\mathrm{T}}(t)]\mathbf{A}(t) \\ &\quad + \mathbf{A}(t)\,\mathrm{E}[\boldsymbol{\Delta}\mathbf{G}(t)]\,\mathrm{E}[\hat{\mathbf{x}}(t-1)\mathbf{v}^{\mathrm{T}}(t-1)]\mathbf{G}^{\mathrm{T}}(t)\mathbf{A}(t) \\ &\quad + \mathbf{A}(t)\,\mathrm{E}[\boldsymbol{\Delta}\mathbf{G}(t)\hat{\mathbf{x}}(t-1)\hat{\mathbf{x}}^{\mathrm{T}}(t-1)\boldsymbol{\Delta}\mathbf{G}^{\mathrm{T}}(t)]\mathbf{A}(t) \\ &\quad + \mu^2\mathbf{D}^{\mathrm{T}}(t)\mathbf{R}_{\mathbf{e}}(t)\mathbf{D}(t)\,, \end{aligned} \tag{11}$$

where $\mathbf{K}_{\mathrm{LMS}}(t) = \mathrm{E}[\mathbf{v}(t)\mathbf{v}^{\mathrm{T}}(t)]$ for the LMS-SRR algorithm.

Following the same steps and statistical assumptions similar to those used in [8], we can derive the following recursion for $\mathbf{K}_{\text{R-LMS}}(t)$ of the R-LMS-SRR algorithm (10):

$$\begin{aligned}\mathbf{K}_{\text{R-LMS}}(t) &= \mathbf{A}(t)\mathbf{G}(t)\mathbf{K}_{\text{R-LMS}}(t-1)\mathbf{G}^{\mathrm{T}}(t)\mathbf{A}(t) \\ &\quad + \lambda\mathbf{A}(t)\mathbf{G}(t)\,\mathrm{E}[\mathbf{v}(t-1)\hat{\mathbf{x}}^{\mathrm{T}}(t-1)]\mathbf{G}^{\mathrm{T}}(t)\mathbf{S}^{\mathrm{T}}\mathbf{S} \\ &\quad + \lambda\mathbf{S}^{\mathrm{T}}\mathbf{S}\mathbf{G}(t)\,\mathrm{E}[\hat{\mathbf{x}}(t-1)\mathbf{v}^{\mathrm{T}}(t-1)]\mathbf{G}^{\mathrm{T}}(t)\mathbf{A}(t) \\ &\quad + \lambda^2\mathbf{S}^{\mathrm{T}}\mathbf{S}\mathbf{G}(t)\,\mathrm{E}[\hat{\mathbf{x}}(t-1)\hat{\mathbf{x}}^{\mathrm{T}}(t-1)]\mathbf{G}^{\mathrm{T}}(t)\mathbf{S}^{\mathrm{T}}\mathbf{S} \\ &\quad + \mu^2\mathbf{D}^{\mathrm{T}}(t)\mathbf{R}_{\mathbf{e}}(t)\mathbf{D}(t)\,. \end{aligned} \tag{12}$$

As it will be discussed, $\mathbf{S}^{\mathrm{T}}\mathbf{S}$, $\mathbf{A}(t)$ and $\boldsymbol{\Delta}\mathbf{G}(t)$ can be interpreted as high-pass filters. Thus, lets start assuming that

$$\lambda\mathbf{S}^{\mathrm{T}}\mathbf{S}\mathbf{G}(t) \simeq \mathbf{A}(t)\boldsymbol{\Delta}\mathbf{G}(t)\,. \tag{13}$$

When integer steps are assumed for the true motion $\mathbf{G}(t)$, we can show that $\hat{\mathbf{G}}(t)$ can be modelled by $\hat{\mathbf{G}}(t) = \tilde{\mathbf{G}}(t)\mathbf{G}(t)$, where $\tilde{\mathbf{G}}(t)$ adds the error to the motion modeled by $\mathbf{G}(t)$ [8]. In this case, (13) becomes

$$\lambda\mathbf{S}^{\mathrm{T}}\mathbf{S}\mathbf{G}(t) \simeq \mathbf{A}(t)[\tilde{\mathbf{G}}(t) - \mathbf{I}]\mathbf{G}(t)\,, \tag{14}$$

and therefore we can assume

$$\lambda\mathbf{S}^{\mathrm{T}}\mathbf{S} \simeq \mathbf{A}(t)[\tilde{\mathbf{G}}(t) - \mathbf{I}]\,. \tag{15}$$

Moving the deterministic matrices $\mathbf{S}^{\mathrm{T}}\mathbf{S}\mathbf{G}(t)$ inside the expectation brackets in (12) and using (15) in the resulting expression, it is easy to show that (12) and (11) become identical for $\mathbf{K}_{\text{R-LMS}}(0) = \mathbf{K}_{\mathrm{LMS}}(0)$.

To see that this similarity is reasonable, note that the main assumption used comes from (15), which substituted in (12) leads to

$$\lambda\mathbf{S}^{\mathrm{T}}\mathbf{S} \simeq \mathbf{A}(t)\{\mathrm{E}[\tilde{\mathbf{G}}(t)] - \mathbf{I}\}\,. \tag{16}$$

In the l.h.s. of (16), $\mathbf{S}$ is a high-pass filter convolution matrix. Now, both $\mathbf{D}(t)$ and $\mathbf{D}^{\mathrm{T}}(t)\mathbf{D}(t)$ act as low-pass filters. Then, $\mathbf{A}(t) = [\mathbf{I} - \mu\mathbf{D}^{\mathrm{T}}(t)\mathbf{D}(t)]$ in the r.h.s. of (16) also acts as a high-pass filter for proper values of μ (certainly for $\mu = 1$). Finally, the warp matrix $\tilde{\mathbf{G}}(t)$ performs a small displacement over a post-multiplied vectorized image [8]. Thus, the effect of $[\tilde{\mathbf{G}}(t) - \mathbf{I}]$ can also be interpreted as a high-pass filtering operation. These arguments show that both sides of (16) perform qualitatively similar processing. Thus, their effects on the behavior of both algorithms should be similar.

Fig. 1 shows the magnitudes of the frequency responses of both sides of (16). Fig. 1(a) is the response of the l.h.s. assuming a Laplacian mask, $\mu = 6$ and $\lambda = 0.01$. $\mathbf{A}(t)$ can not be implemented via a simple convolution, since $\mathbf{D}^{\mathrm{T}}(t)\mathbf{D}(t)$ includes a subsampling followed by an interpolation. Thus, Fig. 1(b) shows an approximation of the frequency response of the r.h.s of (16) for the same step-size as in Fig. 1(a). $\mathrm{E}[\tilde{\mathbf{G}}(t)]$ was estimated from 500 MC simulations. For each realization, $\tilde{\mathbf{G}}(t)$ was generated from random vertical and horizontal displacements modelled as $\mathrm{WGN}(0, 0.5)$. It is clear that the filter responses are both high-pass as anticipated.

As an illustration of the conclusion above, Fig. 2(b) shows the difference between the "house" image (Fig. 2(a)) and its shifted version, considering a displacement of one pixel to the right. The result is a vertical edge detection. Therefore, assuming the registration error as WGN (see [8] for more details about the validity of this assumption in practical situations), it is reasonable to expect the matrix $\mathrm{E}[\tilde{\mathbf{G}}(t)]$ to perform the edge detection in all directions. Fig. 2(c) shows the mean difference image estimated from 100 Monte Carlo (MC) simulations for vertical and horizontal displacements given by a $\mathrm{WGN}(0, 0.5)$ random processes (Figs. 2(b) and (c) had their gray levels inverted and their contrast enhanced for printing purposes).

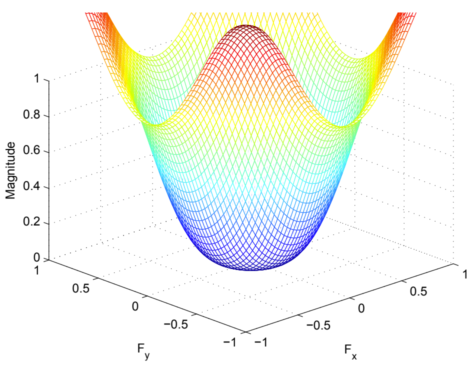

(a)

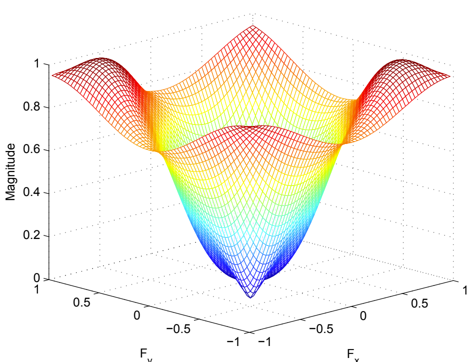

(b)

Fig. 1. Frequency response of the filter performed by: (a) $\lambda \mathbf{S}^{\mathrm{T}}\mathbf{S}$; (b) $\mathbf{A}(t)\{\mathrm{E}[\tilde{\mathbf{G}}(t)] - \mathbf{I}\}$ (approximated).

(a)

(b)

(c)

Fig. 2. High-pass effect caused by registration errors: (a) original "house" image; (b) difference between the "house" image and its one-pixel shifted to the right version; (c) mean difference image considering 100 random displacements.

4. RESULTS

To illustrate the equivalence between the effects of registration errors and regularization in the LMS-SRR algorithm, we devised two simulation examples. Both simulations are for whole image translational movements generated from unit step increments in both vertical and horizontal directions (diagonal camera motion), in the HR grid, at each time instant t. For the R-LMS-SRR algorithm, the movement is assumed known (no registration errors). 128×128 HR and 64×64 LR images were considered. The additive noise vector $\mathbf{e}(t)$ was modelled as a $\mathrm{WNG}(0, 10)$ process. Neumann boundary conditions were considered in the implementation of the warp matrix, in the LMS-SRR algorithm. Registration algorithms from [11] and from [12] were considered.

4.1. Example 1:

This example considers a typical situation where regularization is required. The step-size was $\mu = 6$. $\mathbf{D}(t)$ modeled blurring through a 2×2 mean filter performed over an impulsive subsampling. Fig. 3 shows the spatial mean-square reconstruction errors $\mathrm{tr}(\mathbf{K}_{\text{R-LMS}})$ for the R-LMS-SRR algorithm for $\lambda = 0.01$ and $\lambda = 0.05$. Also shown are the results for the LMS-SRR algorithm with known motion and using two different registration algorithms [11, 12]. Note that R-LMS-SRR with $\lambda = 0.01$ leads to better performance than LMS-SRR with known motion. However, when LMS-SRR is implemented using the registration algorithm from [11], which provides a moderate level of registration error, it outperforms the known motion case and leads to results comparable to those obtained using R-LMS-SRR. For larger registration error levels (obtained using the registration algorithm from [12]), LMS-SRR leads to results similar to those obtained using the over-smoothed ($\lambda = 0.05$) R-LMS-SRR.

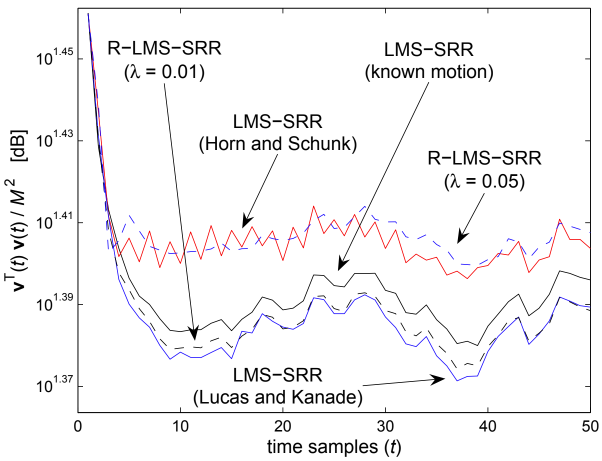

Fig. 3. Spacial mean square reconstruction error considering the R-LMS-SRR and the LMS-SRR algorithms (parameters from Example 1).

4.2. Example 2:

This example presents a situation in which the result is over-smoothed and a smooth restriction degrades the reconstructed image. The step-size is $\mu = 7.8$. $\mathbf{D}(t)$ models blurring as a Gaussian 6×6 low-pass filtering mask with variance 1.0, performed over an impulsive sub-sampling. Fig. 4 shows the spatial mean-square reconstruction errors for the R-LMS-SRR and LMS-SRR algorithms. Known motion case and registration using the algorithm from [11] are considered. As the result with known motion (no regularization) is already smooth, the same regularization factor ($\lambda = 0.01$) that improved the result in the Example 1 now over-smoothes the estimated image. Once again, the results show that the effect of the registration errors is equivalent to a regularization term.

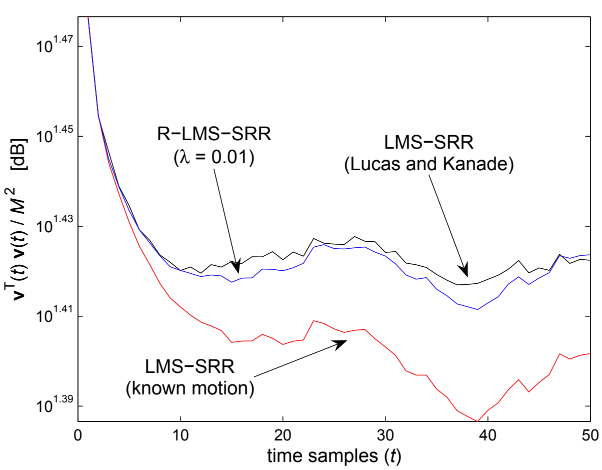

Fig. 4. Spacial mean square reconstruction error considering the R-LMS-SRR and the LMS-SRR algorithms (parameters from Example 2).

5. CONCLUSIONS

This work presented a comparative study of the influences of registration errors and regularization on the performance of the LMS algorithm applied to super-resolution reconstruction. The main conclusions of this work are:

i) Contrary to what is traditionally assumed, a moderate level of registration error may be beneficial for the performance of the LMS-SRR algorithm (depending on the implementation);

ii) The occurrence of moderate registration errors, even in known motion applications, can contribute for reducing computational complexity of the LMS-SRR algorithm by avoiding the need for regularization.

6. REFERENCES

[1] S.C. Park, M.K. Park, and M.G. Kang, "Super-resolution image reconstruction: A technical overview," *IEEE Signal Processing Magazine*, vol. 20, no. 3, pp. 21–36, May 2003.

[2] E.S. Lee and M.G. Kang, "Regularized adaptive high-resolution image reconstruction considering inaccurate subpixel registration," *IEEE Trans. Image Processing*, vol. 12, no. 7, pp. 826–837, July 2003.

[3] M. Elad and A. Feuer, "Superresolution restoration of an image sequence: Adaptive filtering approach," *IEEE Trans. Image Processing*, vol. 8, no. 3, pp. 387–395, Mar. 1999.

[4] D. Capel and A. Zisserman, "Computer vision applied to super resolution," *IEEE Signal Processing Magazine*, vol. 20, no. 3, pp. 75–86, May 2003.

[5] Z. Wang and F. Qi, "Super-resolution video restoration with model uncertainties," *IEEE Int'l Conf. Image Processing*, vol. 2, pp. 853–856, Sept. 2002.

[6] S. Farsiu, D. Robinson, M. Elad, and P. Milanfar, "Fast and robust multiframe super resolution," *IEEE Trans. Image Processing*, vol. 13, no. 10, pp. 1327–1344, Oct. 2004.

[7] G.H. Costa and J.C.M. Bermudez, "On the design of the LMS algorithm for robustness to outliers in super-resolution video reconstruction," *IEEE Int'l Conf. Image Processing*, Oct. 2006.

[8] G.H. Costa and J.C.M. Bermudez, "Statistical analysis of the LMS algorithm applied to super-resolution video reconstruction," *IEEE Int'l Conf. Acoustics, Speech, and Signal Processing*, vol. 3, pp. 101–104, May 2006.

[9] T. Ono, H. Hasegawa, I. Yamanda, and K. Sakaniwa, "An adaptive super-resolution of videos with noise information on camera systems," *IEEE Int'l Conf. Acoustics, Speech, and Signal Processing*, vol. 2, pp. 857–860, Mar. 2005.

[10] G.H. Costa and J.C.M. Bermudez, "A statistical model for the warp matrix in super-resolution reconstruction," *IEEE / SBT Int'l Telecommunication Symposium*, pp. 557–562, Sept. 2006.

[11] B.D. Lucas and T. Kanade, "An iterative image registration technique with an application to stereo vision," *DARPA Image Understanding Workshop*, pp. 121–130, Apr. 1981.

[12] B.K.P. Horn and B.G. Schunck, "Determining optical flow," *Artificial Intelligence*, vol. 17, pp. 185–203, 1981.